Robotics and Autonomous Systems 41 (2002) 257–270

Dynamic modelling, simulation and control of a manipulator with flexible links and joints

B. Subudhi*, A.S. Morris

Department of Automatic Control & Systems Engineering, University of Sheffield, Mappin Street, Sheffield S1 3JD, UK

Received 15 October 2001; received in revised form 17 July 2002
Communicated by F.C.A. Groen

Abstract

The paper presents a dynamic modelling technique for a manipulator with multiple flexible links and flexible joints, based on a combined Euler–Lagrange formulation and assumed modes method. The resulting generalised model is validated through computer simulations by considering a simplified case study of a two-link flexible manipulator with joint elasticity. Controlling such a manipulator is more complex than controlling one with rigid joints because only a single actuation signal can be applied at each joint and this has to control the flexure of both the joint itself and the link attached to it. To resolve the control complexities associated with such an under-actuated flexible link/flexible joint manipulator, a singularly perturbed model has been formulated and used to design a reduced-order controller. This is shown to stabilise the link and joint vibrations effectively while maintaining good tracking performance.

Keywords: Manipulator; Flexible link; Flexible joint; Singular perturbation

1. Introduction

Research on the dynamic modelling and control of flexible manipulators has received increased attention since the last 30 years due to their several advantages over rigid ones [1]. Unlike rigid manipulators, the dynamics of this class of manipulators incorporate the effects of mechanical flexibilities in both the links and joints. Link flexibility is a consequence of the lightweight constructional feature in manipulator arms that are designed to operate at high speed with low inertia. Joint flexibility arises because of the elastic behaviour of the joint transmission elements such as gears and shafts. Thus, flexible manipulators undergo two types of motion, i.e. rigid and flexible motion. Because of the interaction of these motions, the resulting dynamic equations of flexible manipulators are highly complex and, in turn, the control task becomes more challenging compared to that for rigid robots. Therefore, a first step towards designing an efficient control strategy for these manipulators must be aimed at developing accurate dynamic models that can characterise the above flexibilities along with the rigid dynamics.

It has been determined experimentally that joint flexibility exists in most manipulators in the drive transmission systems [9], but little work has been reported on a comprehensive model that describes both link and joint flexibility, particularly for manipulators with more than one link. Coupling effects between a flexible link and flexible joint have been addressed in [4,11]. Two models for a two-link manipulator with both link and joint flexibility have been derived using

* Corresponding author. Fax: +44-114-222-5661.
E-mail address: a.morris@sheffield.ac.uk (B. Subudhi).

the Euler–Lagrange AMM, one with a set of decoupled equations and the other with a set of coupled equations [11]. In a similar work, Lin and Gogate [4] derived the dynamics of a manipulator with flexible links/flexible joints using the Hamilton's principle. These investigations reported that the elasticity in each joint adds an additional degree of freedom to the manipulator, which in turn causes in a large variation in the dynamic behaviour. However, this Lin and Gogate model does not give clear insight into the mechanisms of joint deflection and the effects of structural damping. Also, it does not consider the effects of the payload and structural damping of the links. It has been shown that both the link and the joint flexibility need to be incorporated in the modelling to achieve good trajectory tracking and quick damping of end tip vibrations [4,9,11], because the flexible deformations produced by the joints and the links make it difficult for the end-effector to track a prescribed trajectory accurately.

The modelling of the flexible link/flexible joint manipulator described in this paper is different from that of [4,11] in several ways. First, it follows a systematic approach for deriving the dynamic equations for a *n*-link and *n*-joint manipulator, which is accomplished by the use of two homogeneous transformation matrices describing the rigid and flexible motions, respectively. Second, it gives a clear picture of the joint deflection in terms of discrepancies between link and joint angles. Notably, unlike the model derived by Lin and Gogate [4], the dynamic model of the manipulator in this paper considers the payload and the structural damping of the links.

The paper is organised as follows. In Section 2, a generalised Euler–Lagrange AMM formulation for modelling of a manipulator with flexibilities in both links and joints is presented. The development of dynamic equations for two-link flexible manipulators with flexible joints is then dealt with in Section 3. Subsequently, a two-time-scale singularly perturbed model is proposed in Section 4. Then, based on the two-time-scale separation of the flexible link and flexible joint manipulator dynamics, a controller is designed for tracking and control of link and joint vibrations in Section 5. Results are presented and discussed in Section 6 which show the dynamic behaviour of the manipulator with bang–bang torque input(s) without any control actions and compare this with the performance achieved by employing the proposed controller. The paper is concluded with a brief summary in Section 7.

2. Modelling of a manipulator with multiple flexible links and flexible joints

2.1. Description of the manipulator system

The structure of a multiple flexible links and flexible joints manipulator consisting of n flexible links and n flexible revolute joints is shown in Fig. 1. The links are cascaded in serial fashion and are actuated by rotors and hubs with individual motors. An inertial payload of mass M_{P} and inertia I_{P} is connected to the distal link. The proximal link is clamped and connected to the rotor with a hub.

2.2. Flexible link and flexible joint assembly

The schematic representation for the ith flexible joint and flexible link assembly is shown in Fig. 2. The flexible joint is dynamically simplified as a linear torsional spring that works as a connector between the rotor and the flexible link. α_i and θ_i are the ith rotor and link angular positions, respectively. I_{ri} is the inertia of the ith rotor and hub, where an input torque, $\tau_i(t)$ is applied. G_i is the gear ratio for the ith rotor and k_{si} is the spring constant of the ith flexible joint $(\mathrm{FJ})_i$.

2.3. Assumptions

The following assumptions are made for the development of a dynamic model of the flexible manipulator:

(I) Each link is assumed to be long and slender. Therefore, transverse shear and the rotary inertia effects are negligible.
(II) The motion of each link is assumed to be in the horizontal plane.
(III) Links are considered to have constant cross-sectional area and uniform material properties, i.e. with constant mass density and Young's modulus, etc.
(IV) Each link has a very small deflection.
(V) Motion of the links can have deformations in the horizontal direction only.

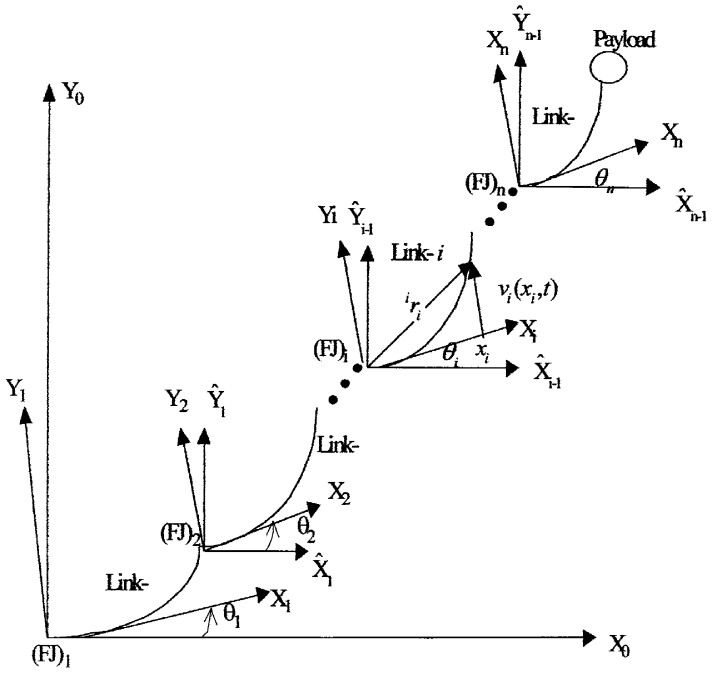

Fig. 1. Multiple flexible links and flexible joints manipulator.

(VI) The kinetic energy of the rotor is mainly due to its rotation only, and the rotor inertia is symmetric about its axis of rotation.
(VII) The backlash in the reduction gear and coulomb friction effects are neglected.

2.4. Kinematics formulation

In this section, the flexible link kinematics is described. Instead of just considering two-links [4,11], the kinematics description is given here for a chain of n serially connected flexible links. The co-ordinate systems of the link are assigned (Fig. 1) referring to the Denavit–Hartenberg (D–H) description [1]. X_0Y_0 is the inertial co-ordinate frame (CF), X_iY_i the rigid body CF associated with the ith link and $\hat{X}_i\hat{Y}_i$ is the flexible moving CF.

Considering revolute joints and motion of the manipulator on a two-dimensional plane, the rigid transformation matrix, $\mathbf{A}_i$, from $X_{i-1}Y_{i-1}$ to X_iY_i is

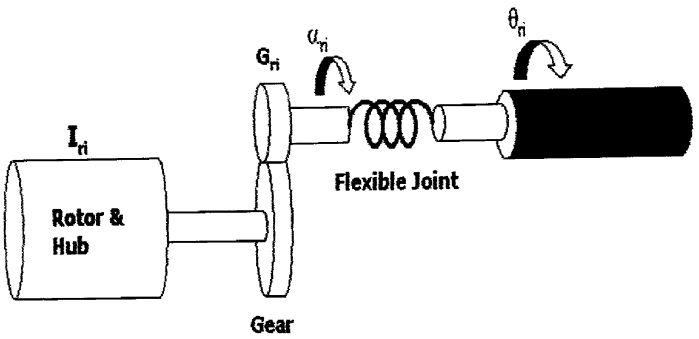

Fig. 2. Schematic of flexible link and flexible joint assembly.

written as [1]

$$\mathbf{A}_i = \begin{bmatrix} \cos\theta_i & -\sin\theta_i \\ \sin\theta_i & \cos\theta_i \end{bmatrix}. \quad (1)$$

On using assumption (IV), the elastic homogenous transformation matrix, $\mathbf{E}_i$, due to the deflection of the link i can be written as [1,10]

$$\mathbf{E}_i = \begin{bmatrix} 1 & -\left.\dfrac{\partial v_i(x_i,t)}{\partial x_i}\right|_{x_i=l_i} \\ \left.\dfrac{\partial v_i(x_i,t)}{\partial x_i}\right|_{x_i=l_i} & 1 \end{bmatrix}, \quad (2)$$

where $v_i(x_i,t)$ is the bending deflection of the ith link at a spatial point x_i ($0 \le x_i \le l_i$) and l_i is the length of the ith link. The global transformation matrix $\mathbf{T}_i$ transforming co-ordinates from X_0Y_0 to X_iY_i follows a recursion as below [1,5]:

$$\mathbf{T}_i = \mathbf{T}_{i-1}\mathbf{E}_{i-1}\mathbf{A}_i = \hat{\mathbf{T}}_{i-1}\mathbf{A}_i, \quad \hat{\mathbf{T}}_0 = \mathbf{I}. \quad (3)$$

Let

$${}^i r_i(x_i) = \begin{Bmatrix} x_i \\ v_i(x_i,t) \end{Bmatrix}$$

be the position vector that describes an arbitrary point along the ith deflected link with respect to its local CF (X_iY_i) and ${}^0r_i$ be the same point referring to X_0Y_0. The position of the origin of $X_{i+1}Y_{i+1}$ with respect to X_iY_i is given by

$${}^i p_{i+1} = {}^i r_i(l_i), \quad (4)$$

and ${}^0p_i$ is its absolute position with respect to X_0Y_0.

Using the global transformation matrix, ${}^0r_i$ and ${}^0p_i$ can be written as

$${}^0r_i = {}^0p_i + \mathbf{T}_i\,{}^i r_i, \qquad {}^0p_{i+1} = {}^0p_i + \mathbf{T}_i\,{}^i p_{i+1}. \quad (5)$$

2.5. Dynamic equations of motion

To derive the dynamic equations of motion for a multiple flexible links and flexible joints manipulator, the total energy associated with the manipulator system needs to be computed using the kinematics formulations explained in Section 2.4 (Fig. 1). In their formulation of a model for a two-flexible links and joints manipulator, Yang and Donath [11] determined the different components of the energy associated with the first and second links separately. They assumed small angular rotation of the links in deriving the kinetic and potential energies due to the motion of the links. Unfortunately, this small angle motion assumption is invalid for a practical manipulator. Also, the approach becomes tedious for deriving equations for a manipulator with many links and joints. Therefore, the derivation of the dynamic equations of the multi-link flexible manipulator presented in this paper does not assume small angular rotation. Instead of adopting only the rigid transformation matrix and then incorporating the elastic deformation of the links, the use of rigid and elastic transformation matrices together makes the development in this formulation more systematic and easy. It also means that the total energy expressions of the multiple links and joints manipulator can be obtained from the ith link and ith rotor energy expressions directly.

The total kinetic energy of the manipulator (T) is given by

$$T = T_{\mathrm{R}} + T_{\mathrm{L}} + T_{\mathrm{PL}}, \quad (6)$$

where T_{R}, T_{L} and T_{PL} are the kinetic energy associated with the rotors, links and the hubs, respectively. Using assumption (VI), the kinetic energy of the ith rotor is given by

$$T_{\mathrm{R}i} = \tfrac{1}{2} J_i \dot{\alpha}_i^2, \quad (7)$$

where $J_i = G_i^2 I_{\mathrm{r}i}$, and $\dot{\alpha}_i$ is the angular velocity of the rotor about the ith principal axis. Therefore, the total kinetic energy for all the n rotors becomes

$$T_{\mathrm{R}} = \tfrac{1}{2}\dot{\boldsymbol{\alpha}}^{\mathrm{T}}\mathbf{J}\dot{\boldsymbol{\alpha}}, \quad (8)$$

where $\boldsymbol{\alpha} = \{\alpha_i\}$ and $\mathbf{J} = \mathrm{diag}(J_i)$, $i = 1, 2, \ldots, n$.

The kinetic energy of a point $r_i(x_i)$ on the ith link can be written as

$$T_{\mathrm{L}i} = \frac{1}{2}\rho_i \int_0^{l_i} {}^0\dot{r}_i^{\mathrm{T}}(x_i)\,{}^0\dot{r}_i(x_i)\,\mathrm{d}x_i, \quad (9)$$

where ρ_i is the linear mass density for the ith link and ${}^0\dot{r}_i(x_i)$ is the velocity vector. The velocity vector can be computed by taking the time derivative of its position (5):

$${}^0\dot{r}_i(x_i) = {}^0\dot{p}_i + \dot{\mathbf{T}}_i\,{}^i r_i(x_i) + \mathbf{T}_i\,{}^i\dot{r}_i(x_i). \quad (10)$$

${}^0\dot{p}_i$ in (10) can be determined using (4) and (5) along with

$${}^i\dot{p}_{i+1} = {}^i\dot{r}_i(l_i). \quad (11)$$

The time derivative of the global transformation matrix $\dot{\mathbf{T}}_i$ can be recursively calculated from [1,5]

$$\dot{\mathbf{T}}_i = \dot{\hat{\mathbf{T}}}_{i-1}\mathbf{A}_i + \hat{\mathbf{T}}_{i-1}\dot{\mathbf{A}}_i, \quad \dot{\hat{\mathbf{T}}}_i = \mathbf{T}_i\mathbf{E}_i + \mathbf{T}_i\dot{\mathbf{E}}_i. \quad (12)$$

Computation of $\dot{\mathbf{A}}_i$ and $\dot{\mathbf{E}}_i$ for (12) can be achieved as follows [5]:

$$\dot{\mathbf{A}}_i = \mathbf{S}\mathbf{A}_i\dot{\theta}_i \quad \text{and} \quad \dot{\mathbf{E}}_i = \mathbf{S}\left.\frac{\partial \dot{v}_i}{\partial x_i}\right|_{x_i=l_i},$$

$$\mathbf{S} = \begin{bmatrix} 0 & -1 \\ 1 & 0 \end{bmatrix}. \quad (13)$$

Evaluation of the transpose and derivative of transpose terms of the velocity vector in (9) can be easily accomplished by using the following identities [5]:

$$\mathbf{A}_i^{\mathrm{T}}\mathbf{A}_i = \mathbf{E}_i^{\mathrm{T}}\mathbf{E}_i = \mathbf{S}^{\mathrm{T}}\mathbf{S} + \mathbf{I} \quad \text{and}$$

$$\mathbf{E}_i^{\mathrm{T}}\dot{\mathbf{E}}_i = (\mathbf{I}v_i'(l_i,t) + \mathbf{S})\dot{v}_i'(l_i,t), \quad (14)$$

$$\mathbf{A}_i^{\mathrm{T}}\dot{\mathbf{A}}_i = \mathbf{S}\dot{\theta}_i, \quad (15)$$

where $\mathbf{I}$ is the identity matrix of appropriate dimensions. After determining the kinetic energy associated with the ith link, the kinetic energy of all the n links can be found as

$$T_{\mathrm{L}} = \sum_{i=1}^{n}\frac{1}{2}\rho_i\int_0^{l_i}\dot{r}_i^{\mathrm{T}}(x_i)\dot{r}_i(x_i)\,\mathrm{d}x_i. \quad (16)$$

Referring to Fig. 1 and the kinematics described in Section 2.4, the kinetic energy associated with the payload can be written as

$$T_{\mathrm{PL}} = \tfrac{1}{2}M_{\mathrm{P}}\dot{p}_{n+1}^{\mathrm{T}}\dot{p}_{n+1} + \tfrac{1}{2}I_{\mathrm{P}}(\dot{\Omega}_n + \dot{v}_n'(l_n))^2, \quad (17)$$

where $\dot{\Omega}_n = \sum_{j=1}^{n}\theta_j + \sum_{k=1}^{n-1}\dot{v}_k'(l_k)$; n being the link number, prime and dot represent the first derivatives with respect to spatial variable x and time, respectively. $\dot{p}_{n+1}$ can be determined using (4) and (5).

Next, neglecting the effects of the gravity, the total potential energy of the system can be written as

$$U = U_{\mathrm{S}} + U_{\mathrm{J}}, \quad (18)$$

where U_{S} and U_{J} are the potential energy resulting from the elastic deflection of the links and joints, respectively. The potential energy due to the deformation of the link i can be written as

$$U_{\mathrm{S}i} = \int_0^{l_i}(\mathrm{EI})_i\left(\frac{\mathrm{d}^2v_i(x_i)}{\mathrm{d}x_i^2}\right)\mathrm{d}x_i. \quad (19)$$

Therefore, for all the n links, it becomes

$$U_{\mathrm{S}} = \sum_{i}^{n}\frac{1}{2}\int_0^{l_i}(\mathrm{EI})_i\left(\frac{\mathrm{d}^2v_i(x_i)}{\mathrm{d}x_i^2}\right)\mathrm{d}x_i. \quad (20)$$

Let the deflection of the ith rotor be $\alpha_i - \theta_i$. Then the elastic potential energy for the ith flexible joint can be written as

$$U_{\mathrm{J}i} = \tfrac{1}{2}k_{si}(\alpha_i - \theta_i)^2. \quad (21)$$

For n-flexible joints, the total elastic potential energy can be written in vector matrix notation as

$$U_{\mathrm{J}} = \tfrac{1}{2}\mathbf{K}_{\mathrm{s}}(\boldsymbol{\alpha} - \boldsymbol{\theta})^{\mathrm{T}}(\boldsymbol{\alpha} - \boldsymbol{\theta}), \quad (22)$$

where $(\mathrm{EI})_i$ is the flexural rigidity of the ith link; $\boldsymbol{\theta} = \{\theta_i\}, i = 1, 2, \ldots, n$ and the stiffness matrix of the joint ($\mathbf{K}_{\mathrm{s}}$) is written as

$$\mathbf{K}_{\mathrm{s}} = \mathrm{diag}(k_{si}). \quad (23)$$

The internal structural damping in each link should also be modelled. Using Rayleigh's dissipation function [6], the dissipation energy for the ith link and jth mode can be written as

$$E_{\mathrm{D}i} = \tfrac{1}{2}d_{ij}\dot{q}_{ij}^2. \quad (24)$$

Therefore for all the n links, each with n_m modes, the total dissipative energy in vector and matrix form can be expressed as

$$E_{\mathrm{D}} = \tfrac{1}{2}\dot{\boldsymbol{q}}^{\mathrm{T}}\mathbf{D}\dot{\boldsymbol{q}}^{\mathrm{T}}, \quad (25)$$

where the damping matrix, $\mathbf{D} = \mathrm{diag}(d_{ij}), i = 1, 2, \ldots, n, j = 1, 2, \ldots, n_m$ (n_m is the number of finite modes (to be explained later)) and d_{ij} is the damping coefficient and the modal displacement vector is $\boldsymbol{q} = \{q_{ij}\}$.

Using assumption (I), the dynamics of the link at an arbitrary spatial point x_i along the link at an instant of time t can be written using Euler–Beam theory [6] as

$$(\mathrm{EI})_i\frac{\partial^4 v_i(x_i,t)}{\partial x_i^4} + \rho_i\frac{\partial^2 v_i(x_i,t)}{\partial t^2} = 0, \quad (26)$$

where ρ_i is the linear mass density of the ith link. Eq. (26) is solved by applying the boundary conditions of the manipulator. Considering a clamped-mass configuration of the manipulator, the boundary conditions can be written as [5,10]

$$v_i(x_i,t)|_{x_i=0} = 0, \quad (27)$$

$$v_i'(x_i,t)|_{x_i=0} = 0, \tag{28}$$

$$(\mathrm{EI})_i \frac{\partial^2 v_i(x_i,t)}{\partial x_i^2}\bigg|_{x_i=l_i} = -I_{\mathrm{E}_i}\frac{\mathrm{d}^2}{\mathrm{d}t^2}\left(\frac{\partial v_i(x_i,t)}{\partial x_i}\bigg|_{x_i=l_i}\right) - M_{\mathrm{DE}_i}\frac{\mathrm{d}^2}{\mathrm{d}t^2}\left(\frac{\partial v_i(x_i,t)}{\partial x_i}\bigg|_{x_i=l_i}\right), \tag{29}$$

$$(\mathrm{EI})_i \frac{\partial^3 v_i(x_i,t)}{\partial x_i^3}\bigg|_{x_i=l_i} = M_{\mathrm{E}_i}\frac{\mathrm{d}^2}{\mathrm{d}t^2}(v_i(x_i,t)|_{x_i=l_i}) + M_{\mathrm{DE}_i}\frac{\mathrm{d}^2}{\mathrm{d}t^2}(v_i(x_i,t)|_{x_i=l_i}), \tag{30}$$

where M_{E_i}, I_{E_i} are the effective mass and moment of inertias at the end of the ith link and M_{DE_i} is the contributions of masses of distal links. These are defined below:

$$M_{\mathrm{E}_i} = \frac{M_{\mathrm{L}_i}}{m_i}, \qquad I_{\mathrm{E}_i} = \frac{I_{\mathrm{L}_i}}{m_i l_i}, \qquad M_{\mathrm{DE}_i} = \frac{M_{\mathrm{D}_i}}{m_i l_i^2}. \tag{31}$$

A finite dimensional solution of (21) can be obtained by means of AMM [6]. Using this method, $v_i(x_i,t)$ can be expressed as a superposition of mode-shapes and time dependent modal displacements:

$$v_i(x,t) = \sum_{j=1}^{n_m} \phi_{ij}(x_i) q_{ij}(t), \tag{32}$$

where $\phi_{ij}(x_i)$ and $q_{ij}(t)$, respectively, are the jth mode shape function and jth modal displacement for the ith link. Substituting for $v_i(x,t)$ from (32) in (26) gives

$$\frac{(\mathrm{EI})_i}{\rho_i \phi_{ij}(x_i)}\frac{\mathrm{d}^4\phi_{ij}(x)}{\mathrm{d}x_i^4} = -\frac{1}{q_{ij}(t)}\frac{\mathrm{d}^2 q_{ij}(t)}{\mathrm{d}t^2} = \omega_{ij}^2. \tag{33}$$

where the constant is ω_{ij}^2. Separating (33) into spatial and temporal parts yields

$$\frac{\mathrm{d}^2((\mathrm{EI})_i(\mathrm{d}^2\phi_{ij}/\mathrm{d}x_i^2))}{\mathrm{d}x_i^2} - \omega_{ij}^2\rho_i\phi_{ij} = 0, \tag{34}$$

$$\frac{\mathrm{d}^2 q_{ij}(t)}{\mathrm{d}t^2} + \omega_{ij}^2 q_{ij}(t) = 0. \tag{35}$$

The solution of (35) is

$$q_{ij}(t) = \exp(\omega_{ij}t), \tag{36}$$

and the solution of (34) is of the form

$$\phi_{ij}(x_i) = N_{ij}[\cos(\beta_{ij}x_i) - \cosh(\beta_{ij}x_i) + \gamma_{ij}\sinh(\beta_{ij}x_i) - \cosh(\beta_{ij}x_i)], \tag{37}$$

where γ_{ij} is given as [10]

$$\gamma_{ij} = \frac{\sin\beta_{ij} - \sinh\beta_{ij} + M_{\mathrm{E}_i}\beta_{ij}(\cos\beta_{ij} - \cosh\beta_{ij}) - M_{\mathrm{DE}_i}\beta_{ij}^2(\sin\beta_{ij} + \sinh\beta_{ij})}{\cos\beta_{ij} + \cosh\beta_{ij} - M_{\mathrm{E}_i}\beta_{ij}(\sin\beta_{ij} - \sinh\beta_{ij}) - M_{\mathrm{DE}_i}\beta_{ij}^2(\cos\beta_{ij} - \cosh\beta_{ij})}, \tag{38}$$

and β_{ij} is the solution of the following equation [10]:

$$\begin{aligned} &1 + \cosh\beta_{ij}l_i\cos\beta_{ij}l_i \\ &- M_{\mathrm{E}_i}\beta_{ij}(\sinh\beta_{ij}l_i - \cosh\beta_{ij}l_i\sin\beta_{ij}l_i) \\ &- I_{\mathrm{E}_i}\beta_{ij}^3(\sinh\beta_{ij}l_i + \cosh\beta_{ij}l_i\sin\beta_{ij}l_i) \\ &+ M_{\mathrm{E}_i}I_{\mathrm{E}_i}\beta_{ij}^4(1 - \cosh\beta_{ij}l_i\sin\beta_{ij}l_i) \\ &+ M_{\mathrm{DE}_i}^2\beta_{ij}^4(1 - \cosh\beta_{ij}l_i\sin\beta_{ij}l_i) \\ &- 2M_{\mathrm{DE}_i}^2\beta_{ij}^4\sinh\beta_{ij}l_i = 0. \end{aligned} \tag{39}$$

N_{ij} are the constants that normalise the mode shape functions such that

$$N_{ij} = \int_0^{l_i}[\phi_{ij}(x_i)]^2\,\mathrm{d}x_i = m_i, \tag{40}$$

where m_i is the mass of the link i. Subsequently, the natural frequency for the jth mode and ith link, ω_{ij}, is determined from the following expression:

$$\beta_{ij}^4 = \frac{\omega_{ij}^2\rho_i}{(\mathrm{EI})_i}. \tag{41}$$

Next, to obtain a closed-form dynamic model of the manipulator, the energy expressions (6)–(25) are used to formulate the Lagrangian $L = T - U$. Using the Euler–Lagrange equation

$$\frac{\partial}{\partial t}\left(\frac{\partial L}{\partial \dot{Q}_i}\right) - \frac{\partial L}{\partial Q_i} + \frac{\partial E_{\mathrm{D}}}{\partial \dot{Q}_i} = F_i \tag{42}$$

with the ith generalised co-ordinate of the system, Q_i, and the corresponding generalised forces, F_i, a set of $4n + 2n_m$ differential equations are obtained. In (42), Q_i, and F_i are defined as follows: $\boldsymbol{Q} = \{Q_i\}$; $\boldsymbol{Q} = \{\boldsymbol{\alpha}, \boldsymbol{\theta}, \boldsymbol{q}\}^{\mathrm{T}}$; $\boldsymbol{F} = \{F_i\}, i = 1, 2, \ldots, 4n + 2n_m$; $\boldsymbol{F} = \{\boldsymbol{\tau}, \mathbf{0}, \mathbf{0}\}^{\mathrm{T}}$; $\boldsymbol{\tau} = \{\tau_i\}$, $i = 1, 2, \ldots, 4n + 2n_m$. After mathematical simplification, these $4n + 2n_m$ dynamic equations can be written in compact form as

$$\mathbf{J}\ddot{\boldsymbol{\alpha}} - \mathbf{K}_{\mathrm{s}}(\boldsymbol{\theta} - \boldsymbol{\alpha}) = \boldsymbol{\tau}, \tag{43}$$

$$\mathbf{M}(\boldsymbol{\theta}, \boldsymbol{q}) \begin{Bmatrix} \ddot{\boldsymbol{\theta}} \\ \ddot{\boldsymbol{q}} \end{Bmatrix} + \begin{Bmatrix} \boldsymbol{f}_1(\boldsymbol{\theta}, \dot{\boldsymbol{\theta}}) \\ \boldsymbol{f}_2(\boldsymbol{\theta}, \dot{\boldsymbol{\theta}}) \end{Bmatrix} + \begin{Bmatrix} \boldsymbol{g}_1(\boldsymbol{\theta}, \dot{\boldsymbol{\theta}}, \boldsymbol{q}, \dot{\boldsymbol{q}}) \\ \boldsymbol{g}_2(\boldsymbol{\theta}, \dot{\boldsymbol{\theta}}, \boldsymbol{q}, \dot{\boldsymbol{q}}) \end{Bmatrix} + \begin{Bmatrix} \mathbf{0} \\ \mathbf{D}\dot{\boldsymbol{q}} \end{Bmatrix} + \begin{Bmatrix} \mathbf{K}_{\mathrm{s}}(\boldsymbol{\theta} - \boldsymbol{\alpha}) \\ \mathbf{K}_{\mathrm{w}}\boldsymbol{q} \end{Bmatrix} = \begin{Bmatrix} \mathbf{0} \\ \mathbf{0} \end{Bmatrix}, \tag{44}$$

where $\mathbf{M}$ is the mass matrix, $\mathbf{J}$ the modified rotor inertia matrix with its elements (J_i), $\boldsymbol{f}_1(\cdot)$ and $\boldsymbol{f}_2(\cdot)$ the vectors containing terms due to coriolis and centrifugal forces, and $\boldsymbol{g}_1(\cdot)$ and $\boldsymbol{g}_2(\cdot)$ are the vectors containing terms due to the interactions of the link angles and their rates with the modal displacements and their rates. The components of the above vectors are determined by using the Christoffel symbols as [5]

$$\boldsymbol{c}^{fg}(\cdot) = \sum_{j=1}^{n+m_d} \sum_{k=1}^{n+m_d} \left(\frac{\partial M_{ij}}{\partial Q_k^{fg}} - \frac{1}{2} \frac{\partial M_{jk}}{\partial Q_i^{fg}} \right) \dot{Q}_j^{fg} \dot{Q}_k^{fg}, \tag{45}$$

where

$$\boldsymbol{c}^{fg}(\cdot) = \begin{Bmatrix} \boldsymbol{f}_1(\cdot) \\ \boldsymbol{f}_2(\cdot) \end{Bmatrix} + \begin{Bmatrix} \boldsymbol{g}_1(\cdot) \\ \boldsymbol{g}_2(\cdot) \end{Bmatrix},$$

and $\boldsymbol{Q}^{fg} = \{Q_i^{fg}\}, i = 1, 2, \ldots, n + m_d$ (m_d being the total number of link-flexure modes). The stiffness matrix due to the distributed flexibility of the links is given by

$$\mathbf{K}_{\mathrm{w}} = \mathrm{diag}(k_{11}, k_{12}, \ldots, k_{1n_m}, k_{21}, k_{22}, \ldots, k_{2n_m}),$$
$$k_{ij} = \omega_{ij}^2 m_i. \tag{46}$$

3. Dynamic model of a manipulator with two flexible links and joints

Using the generalised modelling scheme described in Section 2, equations of motion of a manipulator with two flexible links and flexible joints are derived here. Consider two units of the n-link and n-joint manipulator (Fig. 1) with the first one clamped and a payload connected to the tip of the second link. With a view to obtaining a simplified model with reasonable accuracy, two modes per link are considered.

To derive the kinetic, potential and the dissipative energies associated with the manipulator, the procedure adopted in Section 2 is followed. All these energy expressions can be obtained using (6)–(25) by substituting for links ($i = 1, 2$), for two joints ($i = 1, 2$) and for two modes ($j = 1, 2$).

The solution of the partial differential equation describing the flexible motion of the manipulator can be obtained following the general procedures given in (21)–(35). In this case, the effective masses at the end of the individual links are set as

$$\begin{aligned} M_{\mathrm{E}_1} &= m_2 + M_{\mathrm{P}}, \\ I_{\mathrm{E}_1} &= I_{\mathrm{b}2} + J_2 + I_{\mathrm{P}} + M_{\mathrm{P}} l^2, \\ M_{\mathrm{DE}_1} &= (m_2 l_{\mathrm{c}2} + M_{\mathrm{P}} l_2 \cos\theta_2), \end{aligned} \tag{47}$$

$$M_{\mathrm{E}_2} = M_{\mathrm{P}}, \quad I_{\mathrm{E}_2} = I_{\mathrm{P}} + M_{\mathrm{P}} l^2, \quad M_{\mathrm{D}_2} = 0. \tag{48}$$

It can be seen from (47) that determination of exact mode shapes would require on-line computation of M_{DE_1} as a function of θ_2. However, previous work [5,10] has shown that little error is incurred if the mode shapes are approximated by those corresponding to the undeformed link configuration where $\theta_2 = 0$. Hence, in order to minimise computation time, this approximation was made in this work.

Here, the generalised co-ordinate vector consists of rotor positions (α_1, α_2), link positions (θ_1, θ_2) and modal displacements $(q_{11}, q_{12}, q_{21}, q_{22})$. The generalised force vector is $\boldsymbol{F} = \{\tau_1, \tau_2, 0, 0, \ldots, 0\}^{\mathrm{T}}$, where τ_1 and τ_2 are the torques applied by rotor-1 and rotor-2, respectively. Therefore, the following Euler–Lagrange's equations result, with $i = 1$ and 2 and $j = 1$ and 2:

$$\frac{\mathrm{d}}{\mathrm{d}t} \left(\frac{\partial L}{\partial \dot{\alpha}_i} \right) - \frac{\partial L}{\partial \alpha_i} = \tau_i, \tag{49}$$

$$\frac{\mathrm{d}}{\mathrm{d}t} \left(\frac{\partial L}{\partial \dot{\theta}_i} \right) - \frac{\partial L}{\partial \theta_i} = 0, \tag{50}$$

$$\frac{\mathrm{d}}{\mathrm{d}t} \left(\frac{\partial L}{\partial \dot{q}_{1j}} \right) - \frac{\partial L}{\partial q_{1j}} + \frac{\partial E_{\mathrm{D}}}{\partial \dot{q}_{1j}} = 0, \tag{51}$$

$$\frac{\mathrm{d}}{\mathrm{d}t}\left(\frac{\partial L}{\partial \dot{q}_{2j}}\right) - \frac{\partial L}{\partial q_{2j}} + \frac{\partial E_{\mathrm{D}}}{\partial \dot{q}_{2j}} = 0. \tag{52}$$

The final dynamic equations of motion of the manipulator after algebraic simplifications can be put in concise form as

$$J_{2\times 2}\ddot{\boldsymbol{\alpha}} - \mathbf{K}_{\mathrm{s}2\times 2}(\boldsymbol{\theta} - \boldsymbol{\alpha}) = \boldsymbol{\tau}, \tag{53}$$

$$\begin{aligned}\mathbf{M}_{6\times 6}(\boldsymbol{\theta}, \boldsymbol{q})\begin{Bmatrix}\ddot{\boldsymbol{\theta}}\\ \ddot{\boldsymbol{q}}\end{Bmatrix} &+ \begin{Bmatrix}\boldsymbol{f}_1(\boldsymbol{\theta}, \dot{\boldsymbol{\theta}})\\ \boldsymbol{f}_2(\boldsymbol{\theta}, \dot{\boldsymbol{\theta}})\end{Bmatrix}_{6\times 1}\\ &+ \begin{Bmatrix}\boldsymbol{g}_1(\boldsymbol{\theta}, \dot{\boldsymbol{\theta}}, \boldsymbol{q}, \dot{\boldsymbol{q}})\\ \boldsymbol{g}_2(\boldsymbol{\theta}, \dot{\boldsymbol{\theta}}, \boldsymbol{q}, \dot{\boldsymbol{q}})\end{Bmatrix}_{6\times 1} + \begin{Bmatrix}\mathbf{0}\\ \mathbf{D}_{4\times 4}\dot{\boldsymbol{q}}\end{Bmatrix}\\ &+ \begin{Bmatrix}\mathbf{K}_{\mathrm{s}2\times 2}(\boldsymbol{\theta} - \boldsymbol{\alpha})\\ \mathbf{K}_{\mathrm{w}2\times 2}\boldsymbol{q}\end{Bmatrix} = \begin{Bmatrix}\mathbf{0}\\ \mathbf{0}\end{Bmatrix}.\end{aligned} \tag{54}$$

It may be noted here that, if the joints are assumed to be very stiff, i.e. $k_{si} \to \infty$, then $\alpha = \theta$ and therefore Eqs. (53) and (54) reduce to

$$\begin{aligned}\mathbf{M}_{6\times 6}(\boldsymbol{\theta}, \boldsymbol{q})\begin{Bmatrix}\ddot{\boldsymbol{\theta}}\\ \ddot{\boldsymbol{q}}\end{Bmatrix} &+ \begin{Bmatrix}\boldsymbol{f}_1(\boldsymbol{\theta}, \dot{\boldsymbol{\theta}})_{2\times 1}\\ \boldsymbol{f}_2(\boldsymbol{\theta}, \dot{\boldsymbol{\theta}})_{4\times 1}\end{Bmatrix}_{6\times 1}\\ &+ \begin{Bmatrix}\boldsymbol{g}_1(\boldsymbol{\theta}, \dot{\boldsymbol{\theta}}, \boldsymbol{q}, \dot{\boldsymbol{q}})_{2\times 1}\\ \boldsymbol{g}_2(\boldsymbol{\theta}, \dot{\boldsymbol{\theta}}, \boldsymbol{q}, \dot{\boldsymbol{q}})_{4\times 1}\end{Bmatrix}_{6\times 1} + \begin{Bmatrix}\mathbf{0}\\ \mathbf{D}_{4\times 4}\dot{\boldsymbol{q}}\end{Bmatrix}\\ &+ \begin{Bmatrix}\mathbf{0}\\ \mathbf{K}_{\mathrm{w}4\times 4}\boldsymbol{q}\end{Bmatrix} = \begin{Bmatrix}\boldsymbol{\tau}\\ \mathbf{0}\end{Bmatrix}.\end{aligned} \tag{55}$$

Eq. (55) represents the dynamic model of a two-link flexible manipulator with rigid joints.

4. Two-time-scale singular perturbation model

Control of flexible link manipulators is difficult because they are under-actuated systems in which all modes of flexure in each link have to be controlled by adjusting a single actuating torque. This difficulty is accentuated in the case where both the links and joints are flexible since the actuating torque for each link then has to control the flexure of both the link and its corresponding joint. A successful solution to this control problem in such under-actuated systems has been accomplished previously by using the singular perturbation technique [3]. This essentially uses a perturbation parameter to divide the complex dynamic systems into simpler subsystems at different time scales, and it has been successfully applied for controlling manipulators with either flexible links or flexible joints (but not flexure in both) [2,8]. This previous work is extended in this paper to obtain a singularly perturbed model for a manipulator where there is flexibility in both links and joints simultaneously.

The procedure to formulate a two-time-scale singular perturbation model is as follows. Substituting $\boldsymbol{\delta} = \boldsymbol{\alpha} - \boldsymbol{\theta}$ in (53) and (54), gives

$$\mathbf{J}\ddot{\boldsymbol{\alpha}} + \mathbf{K}_{\mathrm{s}}\boldsymbol{\delta} = \boldsymbol{\tau}, \tag{56}$$

$$\begin{aligned}\mathbf{M}(\boldsymbol{\theta}, \boldsymbol{q})\begin{Bmatrix}\ddot{\boldsymbol{\theta}}\\ \ddot{\boldsymbol{q}}\end{Bmatrix} &+ \begin{Bmatrix}\boldsymbol{f}_1(\boldsymbol{\theta}, \dot{\boldsymbol{\theta}})\\ \boldsymbol{f}_2(\boldsymbol{\theta}, \dot{\boldsymbol{\theta}})\end{Bmatrix} + \begin{Bmatrix}\boldsymbol{g}_1(\boldsymbol{\theta}, \dot{\boldsymbol{\theta}}, \boldsymbol{q}, \dot{\boldsymbol{q}})\\ \boldsymbol{g}_2(\boldsymbol{\theta}, \dot{\boldsymbol{\theta}}, \boldsymbol{q}, \dot{\boldsymbol{q}})\end{Bmatrix}\\ &+ \begin{Bmatrix}\mathbf{0}\\ \mathbf{D}\dot{\boldsymbol{q}}\end{Bmatrix} + \begin{Bmatrix}\mathbf{K}_{\mathrm{s}}\boldsymbol{\delta}\\ \mathbf{K}_{\mathrm{w}}\boldsymbol{q}\end{Bmatrix} = \begin{Bmatrix}\mathbf{0}\\ \mathbf{0}\end{Bmatrix}.\end{aligned} \tag{57}$$

As the inertia matrix $\mathbf{M}(\cdot)$ is positive definite, its inverse, $\mathbf{H}(\cdot)$ can be partitioned. Hence, $\ddot{\boldsymbol{\theta}}$ and $\ddot{\boldsymbol{q}}$ can be determined as follows:

$$\begin{aligned}\ddot{\boldsymbol{\theta}} = &-\mathbf{H}_{11}(\cdot)\boldsymbol{f}_1(\cdot) - \mathbf{H}_{11}(\cdot)\boldsymbol{g}_1(\cdot) - \mathbf{H}_{12}(\cdot)\boldsymbol{g}_2(\cdot)\\ &-\mathbf{H}_{12}(\cdot)\boldsymbol{f}_2(\cdot) + \mathbf{H}_{11}(\cdot)\mathbf{K}_{\mathrm{s}}\boldsymbol{\delta}\\ &-\mathbf{H}_{12}(\cdot)\mathbf{K}_{\mathrm{w}}\boldsymbol{q} - \mathbf{H}_{12}(\cdot)\mathbf{D}\dot{\boldsymbol{q}},\end{aligned} \tag{58}$$

$$\begin{aligned}\ddot{\boldsymbol{q}} = &-\mathbf{H}_{21}(\cdot)\boldsymbol{f}_1(\cdot) - \mathbf{H}_{21}(\cdot)\boldsymbol{g}_1(\cdot)\\ &-\mathbf{H}_{22}(\cdot)\boldsymbol{f}_2(\cdot) - \mathbf{H}_{22}(\cdot)\boldsymbol{g}_2(\cdot)\\ &-\mathbf{H}_{22}(\cdot)\mathbf{K}_{\mathrm{w}}\boldsymbol{q} + \mathbf{H}_{21}(\cdot)\mathbf{K}_{\mathrm{s}}\boldsymbol{\delta} - \mathbf{H}_{22}(\cdot)\mathbf{D}\dot{\boldsymbol{q}}.\end{aligned} \tag{59}$$

Subtracting $\mathbf{J}\ddot{\boldsymbol{\theta}}$ from both the sides of (53),

$$\ddot{\boldsymbol{\delta}} = \ddot{\boldsymbol{\alpha}} - \ddot{\boldsymbol{\theta}} = -\mathbf{J}^{-1}\mathbf{K}_{\mathrm{s}}\boldsymbol{\delta} + \mathbf{J}^{-1}\boldsymbol{\tau} - \ddot{\boldsymbol{\theta}}. \tag{60}$$

Now, define a common scale factor k_{c}, which is the minimum of all the stiffness constants, i.e. $k_{\mathrm{c}} = \min(k_{11}, k_{12}, k_{21}, k_{22}, k_{\mathrm{s}1}, k_{\mathrm{s}2})$. With this common scale factor, $\mathbf{K}_{\mathrm{s}}$ and $\mathbf{K}_{\mathrm{w}}$ can be scaled by k_{c} such that, $\tilde{\mathbf{K}}_{\mathrm{s}} = (1/k_{\mathrm{c}})\mathbf{K}_{\mathrm{s}}$ and $\tilde{\mathbf{K}}_{\mathrm{w}} = (1/k_{\mathrm{c}})\mathbf{K}_{\mathrm{w}}$. Defining $\boldsymbol{\xi}_{\boldsymbol{q}} = k_{\mathrm{c}}\boldsymbol{q}$, $\boldsymbol{\xi}_{\boldsymbol{\delta}} = k_{\mathrm{c}}\boldsymbol{\delta}$, $\mu = (1/k_{\mathrm{c}})$ and substituting, $\boldsymbol{q} = \mu\boldsymbol{\xi}_{\boldsymbol{q}}$ and $\boldsymbol{\delta} = \mu\boldsymbol{\xi}_{\boldsymbol{\delta}}$ into (58)–(60) gives

$$\begin{aligned}\ddot{\boldsymbol{\theta}} = &-\mathbf{H}_{11}(\theta, \mu\xi_{\boldsymbol{q}})\boldsymbol{f}_1(\theta, \dot{\theta}) - \mathbf{H}_{11}(\theta, \mu\xi_{\boldsymbol{q}})\boldsymbol{g}_1(\theta, \dot{\theta})\\ &-\mathbf{H}_{12}(\theta, \mu\xi_{\boldsymbol{q}})\boldsymbol{g}_2(\theta, \dot{\theta}, \mu\xi_{\boldsymbol{q}}, \mu\dot{\xi}_{\boldsymbol{q}})\\ &-\mathbf{H}_{12}(\theta, \mu\xi_{\boldsymbol{q}})\boldsymbol{f}_2(\theta, \dot{\theta}) + \mathbf{H}_{11}(\theta, \mu\xi_{\boldsymbol{q}})\mathbf{K}_{\mathrm{s}}\boldsymbol{\delta}\\ &-\mathbf{H}_{12}(\theta, \mu\xi_{\boldsymbol{q}})\mathbf{K}_{\mathrm{w}}\boldsymbol{q} - \mathbf{H}_{12}(\theta, \mu\xi_{\boldsymbol{q}})\mathbf{D}\dot{\boldsymbol{q}},\end{aligned} \tag{61}$$

$$\begin{aligned}\mu\ddot{\xi}_q = &-\mathbf{H}_{21}(\theta,\mu\xi_q)\boldsymbol{f}_1(\theta,\dot{\theta}) - \mathbf{H}_{21}(\theta,\mu\xi_q)\boldsymbol{g}_1(\theta,\dot{\theta})\\ &-\mathbf{H}_{21}(\theta,\mu\xi_q)\boldsymbol{g}_2(\theta,\dot{\theta},\mu\xi_q,\mu\dot{\xi}_q)\\ &-\mathbf{H}_{22}(\theta,\mu\xi_q)\boldsymbol{f}_2(\theta,\dot{\theta}) + \mathbf{H}_{21}(\theta,\mu\xi_q)\mathbf{K}_s\boldsymbol{\delta}\\ &-\mathbf{H}_{22}(\theta,\mu\xi_q)\mathbf{K}_w\boldsymbol{q} - \mathbf{H}_{22}(\theta,\mu\xi_q)\mathbf{D}\dot{\boldsymbol{q}}, \qquad (62)\end{aligned}$$

$$\mu\xi_\delta = -\mathbf{J}^{-1}\tilde{\mathbf{K}}_s\xi_\delta + \mathbf{J}^{-1}\tau - \ddot{\boldsymbol{\theta}}. \qquad (63)$$

To derive the boundary layer correction, μ is set to zero in (61)–(63) and on solving for $\bar{\xi}_q$ and $\bar{\xi}_\delta$ yields

$$\bar{\xi}_\delta = \tilde{\mathbf{K}}_s^{-1}(\bar{\tau} - \mathbf{J}\ddot{\bar{\theta}}), \qquad (64)$$

$$\begin{aligned}\bar{\xi}_q = &\tilde{\mathbf{K}}_w^{-1}\mathbf{H}_{22}^{-1}[-\mathbf{H}_{21}(\bar{\theta},\mathbf{0})f_1(\bar{\theta}\dot{\bar{\theta}})\\ &-\mathbf{H}_{22}(\bar{\theta},\mathbf{0})\boldsymbol{f}_2(\bar{\theta},\dot{\bar{\theta}}) - \mathbf{H}_{21}(\bar{\theta},\mathbf{0})(\bar{\tau} - \mathbf{J}\ddot{\bar{\theta}})],\end{aligned} \qquad (65)$$

where overbar denotes the value of a variable at $\mu = 0$. Applying the two-time-scale perturbation technique [3,8], the slow and fast subsystems can be obtained as follows:

Slow subsystem:

$$\ddot{\bar{\theta}} = (\mathbf{M}_{11} + \mathbf{J})^{-1}\{-\boldsymbol{f}_1(\bar{\theta},\dot{\bar{\theta}}) + \bar{\tau}\}. \qquad (66)$$

Fast subsystem at a fast time scale, $t_f = t/\varepsilon$ *with* $\varepsilon = \sqrt{\mu}$:

$$\dot{\boldsymbol{x}}_f = \mathbf{A}_f\boldsymbol{x}_f + \mathbf{B}_f\boldsymbol{\tau}_f, \qquad (67)$$

where

$$\mathbf{A}_f = \begin{bmatrix} \mathbf{0} & \mathbf{0} & \mathbf{I} \\ -\mathbf{H}_{22}\tilde{\mathbf{K}}_w & \mathbf{H}_{21}\tilde{\mathbf{K}}_s & \mathbf{0} \\ \mathbf{0} & \mathbf{J}^{-1}\tilde{\mathbf{K}}_s & \mathbf{0} \end{bmatrix},$$

$$\mathbf{B}_f = \begin{bmatrix} \mathbf{0} \\ \mathbf{J}^{-1}\tilde{\mathbf{K}}_s \end{bmatrix}, \qquad \boldsymbol{x}_f = [\,\eta_q^1 \quad \eta_a^1 \quad \eta_q^2 \quad \eta_a^2\,]^T,$$

$$\boldsymbol{n}_q^1 = \boldsymbol{\xi}_q - \bar{\xi}_q, \qquad \boldsymbol{n}_q^2 = \varepsilon\dot{\boldsymbol{\xi}}_q,$$

$$\boldsymbol{n}_a^1 = \boldsymbol{\xi}_\delta - \bar{\xi}_\delta, \qquad \boldsymbol{n}_a^2 = \varepsilon\dot{\boldsymbol{\xi}}_\delta,$$

0 and **I** matrices are of appropriate dimensions.

5. Design of composite control scheme

Fig. 3 gives the structure for the composite controller based on the two-time-scale model of the manipulator with two flexible links and two flexible joints given in (53) and (54). Following the composite control strategy, the net torque, $\boldsymbol{\tau}$ can be determined as [3]

$$\boldsymbol{\tau} = \bar{\boldsymbol{\tau}} + \boldsymbol{\tau}_f, \qquad (68)$$

where $\bar{\boldsymbol{\tau}}$ is the slow control and $\boldsymbol{\tau}_f$ is the fast control. The controller for the slow subsystem can be designed according to the computed torque control technique, which can be written as

$$\begin{aligned}\bar{\boldsymbol{\tau}} = &(\mathbf{M}_{11} + \mathbf{J})\{\ddot{\boldsymbol{\theta}}_d(t) + \boldsymbol{K}_{ps}(\boldsymbol{\theta}_d(t) - \bar{\boldsymbol{\theta}}(t))\\ &+\mathbf{K}_{vs}(\dot{\boldsymbol{\theta}}_d(t) - \dot{\bar{\boldsymbol{\theta}}}(t))\},\end{aligned} \qquad (69)$$

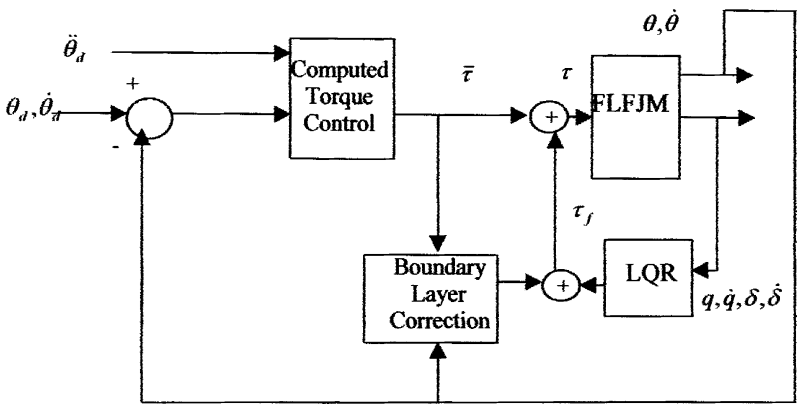

Fig. 3. Composite control scheme.

where $\mathbf{K}_{ps}$ and $\mathbf{K}_{vs}$ are the diagonal position and velocity gain matrices of the controller and $\boldsymbol{\theta}_d(t)$ are the desired trajectories of the two links. As the fast subsystem (67) is completely controllable, a fast state feedback control can be devised to force its states $\boldsymbol{x}_f$ to zero. This is given by

$$\boldsymbol{\tau}_f = \mathbf{K}_{pf}\boldsymbol{x}_f + \mathbf{K}_{vf}\frac{d\boldsymbol{x}_f}{dt_f}, \tag{70}$$

where the feedback gains $\mathbf{K}_{pf}$ and $\mathbf{K}_{vf}$ are obtained through optimising the cost function using an LQR approach [7].

6. Implementation, results and discussions

The dynamic equations (53) and (54) characterising the behaviour of the two-link flexible manipulator with flexible joints derived in Section 3 are verified in this section by undertaking a computer simulation using the fourth-order Runge–Kutta integration method at a sampling rate of 1 ms. The physical parameters of the manipulator were taken from [5] and are given in Table 1. Both the links and rotors are considered to have the same dimensions. The manipulator was excited with symmetric bang–bang torque inputs applied at the rotors, each of 0.2 N m amplitude and 0.5 s width (see Fig. 4(a)). The responses of the manipulator (without control) are presented in Figs. 4–6 and show the difference between the flexible link/flexible joint model and a flexible link/rigid joint model. It is observed from Fig. 4(b) and (c) that, due to the joint elasticity, the links exhibit more oscillatory behaviour than they would do if the joints were rigid. The amplitudes of the first and second modes of vibrations for both the links (Figs. 4(d), 5(a), 5(b) and 5(c)) and the tip deflections of the links (Figs. 5(d) and 6(a)) are greater with flexible joints. Also the oscillations

Table 1
Parameters of the manipulator

Parameter	Symbol	Value
Mass density	ρ	0.2 kg m^{-1}
Flexural rigidity	EI	1.0 N m^2
Length	l	0.5 m
Rotor and hub inertia	I_r	0.02 kg m^2
Gear ratio	G	1
Stiffness constant	k_s	100 N m/rad
Payload mass	M_P	0.1 kg
Payload inertia	I_P	0.005 kg m^2

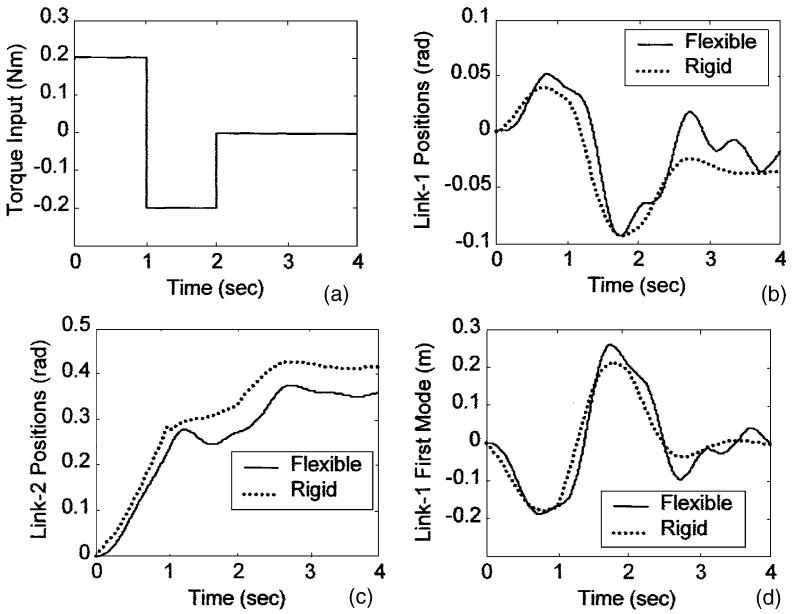

Fig. 4. Responses of the manipulator: (a) torque input; (b) link-1 angular positions; (c) link-2 angular positions; (d) link-1 first mode trajectories.

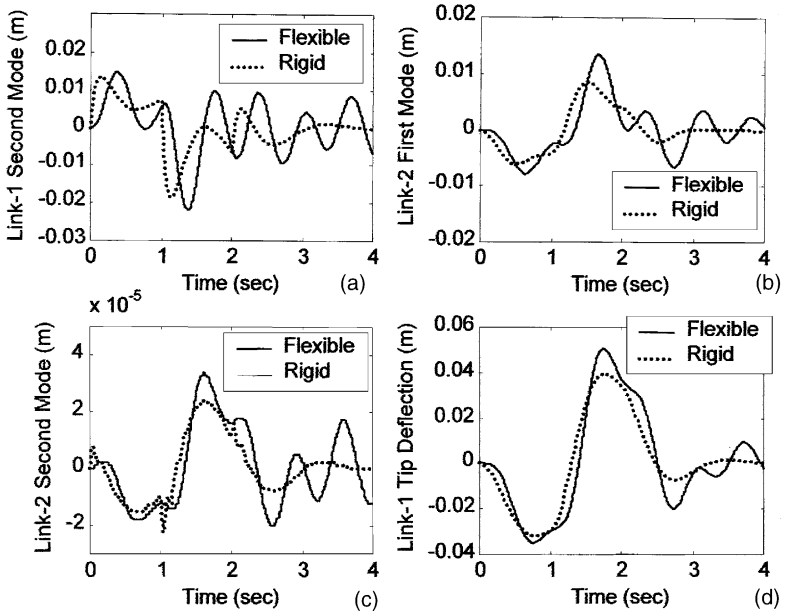

Fig. 5. Responses of the manipulator: (a) link-1 second mode of vibration; (b) link-2 first mode of vibration; (c) link-2 second mode of vibration; (d) link-1 tip deflection.

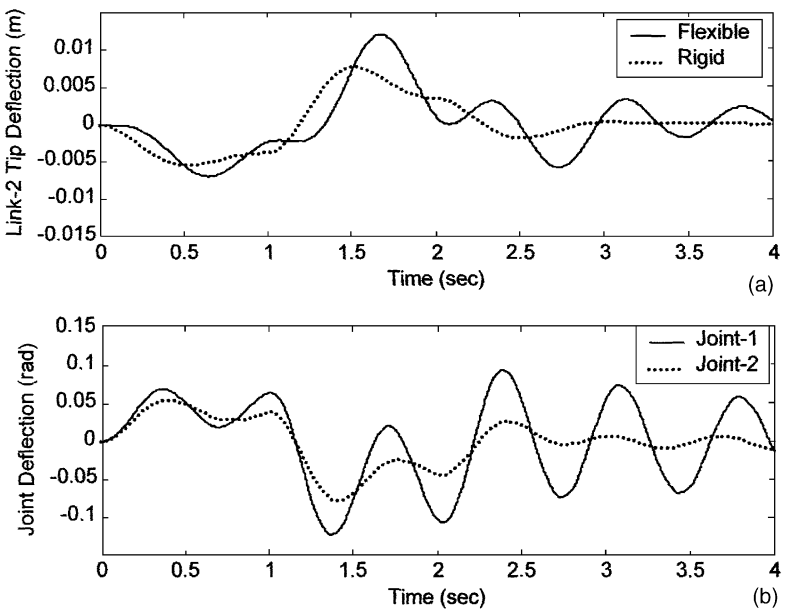

Fig. 6. (a) Tip and (b) joint deflection trajectories of the manipulator.

in modal vibrations and tip deflections with flexible joints do not decay with time, unlike the modes of vibration and the tip deflection responses with rigid joints. The elasticity in the joints excites greater first and second mode vibration in both links, leading to significant tip deflections of the links both in amplitude and frequency (Figs. 5(d) and 6(a)). Fig. 6(b) shows that both the link angular positions have deviations from their respective rotor positions. Thus, it is clear that joint flexibility significantly affects the link vibrations. This necessitates a suitable controller to damp out the link and joint vibrations simultaneously to achieve good tracking performance.

The tracking performance of the singular perturbation based composite controller applied to a manipulator with two flexible links and two flexible joints was verified with the desired trajectories defined as

$$\boldsymbol{\theta}_{\mathrm{d}}(t) = \boldsymbol{\theta}_0(t) + \left(6\frac{t^5}{t_{\mathrm{d}}^5} - 15\frac{t^4}{t_{\mathrm{d}}^4} + 10\frac{t^3}{t_{\mathrm{d}}^3}\right)(\boldsymbol{\theta}_{\mathrm{f}} - \boldsymbol{\theta}_0), \tag{71}$$

where $\boldsymbol{\theta}_{\mathrm{d}}(t) = \{\theta_{\mathrm{d1}}(t), \theta_{\mathrm{d2}}(t)\}^{\mathrm{T}}$, $\boldsymbol{\theta}_0 = \{0, 0\}^{\mathrm{T}}$ are the initial positions of the links, $\boldsymbol{\theta}_{\mathrm{f}} = \{\pi/2, \pi/6\}^{\mathrm{T}}$ the final positions, and t_{d} is the time taken to reach the final position which is taken as 2 s. The gains for the slow and fast control components of the composite singular perturbation control were set as

$$\mathbf{K}_{\mathrm{ps}} = \mathrm{diag}(5.0, 5.0), \qquad \mathbf{K}_{\mathrm{vs}} = \mathrm{diag}(2.0, 2.0),$$

$$\mathbf{K}_{\mathrm{pf}} = \begin{bmatrix} 4.0 & 2.5 & -1.3 & 1.8 & 28.3 & -58.26 \\ 0.0 & -1.0 & -1.0 & 0.0 & 5.6 & 8.6 \end{bmatrix},$$

$$\mathbf{K}_{\mathrm{vf}} = \begin{bmatrix} 8.0 & -37.2 & -1.5 & 28.8 & 126.0 & 58.03 \\ 4.0 & 0.0 & 5.0 & -3.0 & -8.6 & 14.7 \end{bmatrix}.$$

The controller performances are shown in Figs. 7 and 8. It can be seen from Fig. 7(a) that good tracking performance is achieved through the application of the proposed controller. Figs. 7(c), 7(d), 8(a) and 8(b) show that first and second mode of vibration of both the links are well damped. The tip and joint deflections are also suppressed effectively while tracking the desired trajectories (see Figs. 7(b) and 8(c)). The control signals generated for rotor-1 and rotor-2 using the composite controller are shown in Fig. 8(d).

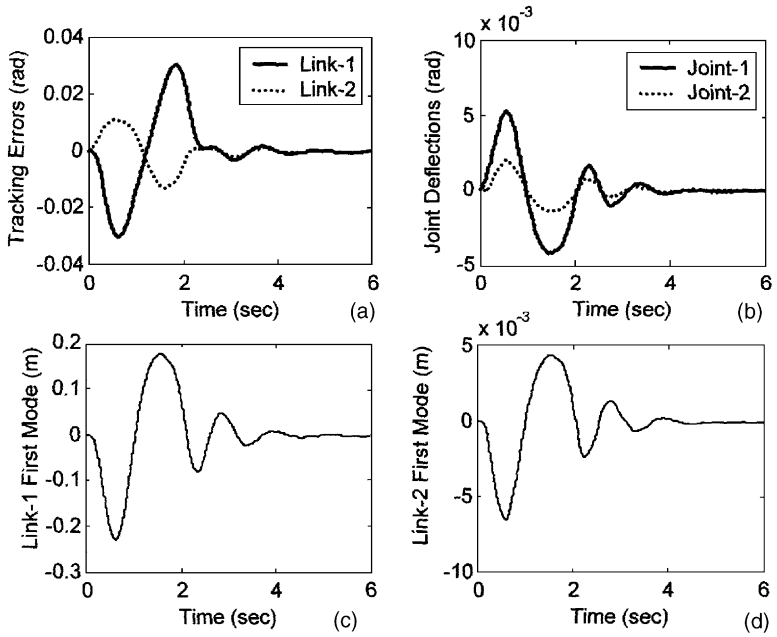

Fig. 7. Controller performance: (a) tracking desired trajectories; (b) damping joint deflections; (c) link-1 first modal vibration; (d) link-2 second mode trajectory.

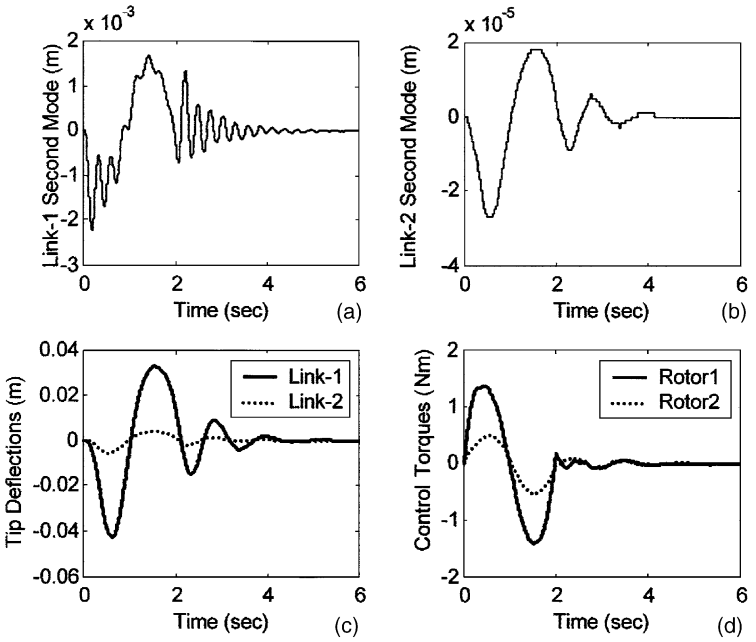

Fig. 8. Controller performance: (a) link-1 second mode trajectory; (b) link-2 second mode trajectory; (c) tip deflections control; (d) control torque signals generated.

7. Conclusions

A generalised modelling framework has been described to obtain the closed-form dynamic equations of motion for a multi-link manipulator considering flexibility in the links and the joints by using the Euler–Lagrange principle and assumed modes discretisation technique. Unlike the models derived in [11], the model presented in this paper for a multi-link manipulator with both link and joint flexibility is a generalised one. This is very useful for the study of manipulators with multiple links and joints that are all flexible. As compared to the model formulation in [4], the proposed model is more complete in the sense that it considers the effects of payload and structural damping of the links. The general model formulation can be exploited to obtain the closed-form dynamic models for practical flexible manipulators with any number of links. The model equations have been verified using bang–bang torque inputs in a two-link manipulator, and the model responses have been discussed. The two-time-scale separation of the complex dynamics of the flexible link and flexible joint manipulator makes the control design simpler. With application of the proposed controller to a flexible link and flexible joint manipulator, good tracking is performed and both link and joint vibrations are suppressed effectively.

References

[1] W.J. Book, Recursive Lagrangian dynamics of flexible manipulator arms, International Journal of Robotics Research 3 (3) (1984) 87–101.
[2] K. Khorasani, Adaptive control of flexible joint-robots, IEEE Transactions on Robotics and Automation 8 (2) (1992) 251–267.
[3] P.V. Kokotovic, H.K. Khalil, J. O'Reilly, Singular perturbation methods in control: analysis and design, in: SIAM Classics in Applied Mathematics, vol. 25, Society of Industrial and Applied Mathematics, Philadelphia, PA, USA, 1999.
[4] Y.J. Lin, S.D. Gogate, Modelling and motion simulation of an *n*-link flexible robot with elastic joints, in: Proceedings of the International Symposium on Robotics and Manufacturing, Santa Barbara, CA, 1989, pp. 39–43.
[5] A. De Luca, B. Siciliano, Closed-form dynamic model of planar multi-link lightweight robots, IEEE Transactions on Systems, Man, and Cybernetics 21 (4) (1991) 826–839.
[6] L. Meirovitch, Analytical Methods in Vibration, Macmillan, New York, 1967.
[7] K. Ogata, Modern Control Engineering, Prentice-Hall International, Upper Saddle River, NJ, 1997.

[8] B. Siciliano, W.J. Book, A singular perturbation approach to control of lightweight flexible manipulators, International Journal of Robotics Research 7 (4) (1988) 79–90.
[9] L.M. Sweet, M.C. Good, Re-definition of the robot motion control problem: effects of plant dynamics, drive systems, constraints and user requirement, in: Proceedings of the 23rd IEEE Conference on Decision and Control, Las Vegas, NV, 1984, pp. 724–731.
[10] R. Theodore, A. Ghosal, Comparison of the assumed modes and finite element models for flexible multi-link manipulators, International Journal of Robotics Research 14 (2) (1995) 91–111.
[11] G.B. Yang, M. Donath, Dynamic model of a two-link robot manipulator with both structural and joint flexibility, in: Proceedings of the ASME 1988 Winter Annual Meeting, Chicago, IL, 1988, pp. 37–44.

Bidyadhar Subudhi received a BSc (Engg.) degree from the Regional Engineering College, Rourkela, India in 1988 and a Master of Technology degree from the Indian Institute of Technology, Delhi, India in 1993. Subsequently, he was awarded a PhD degree from the University of Sheffield in 2002. Currently he is an Assistant Professor in the Department of Electrical Engineering in the Indira Gandhi Institute of Technology, Sarang, India. His research interests include robotics, fuzzy logic, neural networks and control systems. He is an author of 10 journal papers and 15 conference papers. He is a member of the Institution of Engineers (India) and IEEE (USA).

Alan S. Morris was born and educated in England and graduated with a BEng degree in Electrical and Electronic Engineering from Sheffield University in 1969. Following 5 years employment with British Steel as a research and development engineer in control system applications, he returned to Sheffield University to carry out research in electric arc furnace control, for which he was awarded the PhD degree in 1978. Since that time, he has been employed as a lecturer, and more recently senior lecturer, at Sheffield. His main research interests lie in robotics, and he is now the author of over 120 refereed research papers. Professionally, he is a Fellow of both the Institution of Electrical Engineers and the Institute of Measurement and Control.